



**HAL**  
open science

# A model reduction method to analyze the dynamic behavior of vibrating structures with uncertain parameters

Duc-Think Kieu, Marie-Laure Gobert, Sébastien Berger, Jean-Mathieu Mencik

► **To cite this version:**

Duc-Think Kieu, Marie-Laure Gobert, Sébastien Berger, Jean-Mathieu Mencik. A model reduction method to analyze the dynamic behavior of vibrating structures with uncertain parameters. Surveillance, Vishno and AVE conferences, INSA-Lyon, Université de Lyon, Jul 2019, Lyon, France. hal-02190163

**HAL Id: hal-02190163**

**<https://hal.science/hal-02190163v1>**

Submitted on 22 Jul 2019

**HAL** is a multi-disciplinary open access archive for the deposit and dissemination of scientific research documents, whether they are published or not. The documents may come from teaching and research institutions in France or abroad, or from public or private research centers.

L'archive ouverte pluridisciplinaire **HAL**, est destinée au dépôt et à la diffusion de documents scientifiques de niveau recherche, publiés ou non, émanant des établissements d'enseignement et de recherche français ou étrangers, des laboratoires publics ou privés.

# A model reduction method to analyze the dynamic behavior of vibrating structures with uncertain parameters

Duc Think Kieu, Marie-Laure Gobert, Sébastien Berger, Jean-Mathieu Mencik

INSA CVL, Univ. Orléans, Univ. Tours, LaMé EA 7494, F-41034, 3 Rue de la Chocolaterie,  
CS 23410, 41034 Blois Cedex, France  
sebastien.berger@insa-cvl.fr

## Abstract

Assessing the dynamic response of vibrating structures which are described by means of finite element (FE) models with many degrees of freedom (DOFs) is usually computationally cumbersome. The fact that the manufacturing process and the material properties of structures are usually subject to variability means a dispersion of the physical parameters which can be important. The parameters are therefore considered as uncertain DOFs, which makes FE models more complex. The Monte Carlo (MC) method is commonly used to analyze the propagation of uncertainties through FE modeling. However, it requires a large number of simulations which are therefore very cumbersome in terms of CPU times. This work aims at developing a low cost computational strategy to compute the harmonic response of vibrating structures having uncertain parameters. The strategy works by considering the Craig-Bampton method to reduce the physical DOFs of a FE model [1]. Also, a sparse Polynomial Chaos (sPC) expansion is considered to describe the propagation of uncertainties and estimate the Quantities of Interest (QoIs), e.g., the displacement at some measurement points, or an energy quantity. In this work, the sPC expansion is applied through a non-intrusive method, which requires a non-negligible number of simulations of the FE model to be performed to estimate the sPC coefficients, and further the statistics (i.e., mean and variance) of the QoIs. The probability law of the QoIs can be obtained by considering the sPC expansions along with the MC method with 10000 trials. The strategy is here applied to model an academic structure composed of three rectangular Kirchhoff-Love plates made up of various materials and connected together across one of their edges by means of a lineic density of springs with an uncertain stiffness. Comparisons with the results obtained from a reference MC solution involving 10000 simulations of the FE model show good agreement and substantial reduction of the computational effort. The influence of the Craig-Bampton reduction method on the estimation of the QoIs of the FE model is discussed through numerical comparisons.

## 1 Introduction

Applying the FE method to perform the dynamic analysis of complex industrial structures usually involves models characterized by large numbers of DOFs and leads to large computational costs. It may therefore be necessary to reduce the size of the models to solve. One of the efficient model reduction strategies is the well-established Craig-Bampton method, which is based on the projection of the system internal DOFs onto bases of reduced sizes [1, 2].

In addition, the effect of uncertainties are of growing concern in the analysis and design of engineering structures. These uncertainties in the parameters of the system result from the inevitable variability in the manufacturing process of the structures and the fact that the material properties of the structures can change with time [3, 4]. Taking into account these uncertainties in the dynamic analysis of vibrating structures is therefore a crucial issue. The classic MC approach is usually used to analyze the propagation of uncertainties, and involves a large number of FEM evaluations for various sets of values of the uncertain parameters. For complex industrial systems owning a large number of DOFs and/or uncertain parameters, the computational cost associated with this method becomes prohibitive. Polynomial chaos (PC) expansions have proved efficient to solve this issue, among which sparse PC expansions (sPC) [6, 7, 8] are of particular interest when a large number of uncertain parameters is at stake. For instance, Kieu et al. [5] have recently applied sPC expansions to analyze the stability of a clutch system having uncertain parameters. In that study, comparisons with the generalized polynomial

chaos (gPC) and the multi-element generalized polynomial chaos (ME-gPC) previously applied to the same clutch system [9] shew that the sPC expansions ensured substantial time reduction with respect to the other PC expansions, while providing a high accuracy of the results.

The aim of this paper is to associate an sPC expansion to a CB model reduction in order to reduce the computational costs in the analysis of the dynamic behavior of a vibrating structure having uncertain parameters. The Craig-Bampton method is briefly recalled in section 2, and the building of a sparse PC expansion is detailed in section 3. The method is then applied to a system consisting of several plates connected with spring of uncertain stiffness. The details of the model and the results are finally given in section 4.

## 2 The Craig-Bampton method

The Craig Bampton method [1] aims at reducing the sizes of FE models involving large numbers of DOFs. Within the FE framework, the equation of motion of a structure is

$$[M]\{\ddot{q}\} + [K]\{q\} = \{F\}, \quad (1)$$

where  $[M]$  and  $[K]$  denote respectively the mass and stiffness matrices of the structure,  $\{q\}$  the vector of displacements and  $\{F\}$  the vector of external forces. Considering harmonic forces and distinguishing the internal DOFs  $q_I$  from the boundary DOFs  $q_B$ , the above equation may be rewritten as:

$$-\omega^2 \begin{bmatrix} M_{BB} & M_{BI} \\ M_{IB} & M_{II} \end{bmatrix} \begin{Bmatrix} q_B \\ q_I \end{Bmatrix} + \begin{bmatrix} K_{BB} & K_{BI} \\ K_{IB} & K_{II} \end{bmatrix} \begin{Bmatrix} q_B \\ q_I \end{Bmatrix} = \begin{Bmatrix} F_B \\ F_I \end{Bmatrix}. \quad (2)$$

In the classical FE procedure, the unknown DOFs are obtained by inverting the above system, which can be cumbersome in terms of computational time if the number of DOFs involved is important. The CB method consists in decomposing the vector of internal DOFs onto a basis of static and fixed interface modes as follows:

$$\begin{Bmatrix} q_B \\ q_I \end{Bmatrix} = \begin{bmatrix} I & 0 \\ X_{st} & X_{el} \end{bmatrix} \begin{Bmatrix} q_B \\ \alpha \end{Bmatrix} \quad (3)$$

where  $X_{st}$  is the matrix of static modes, which are computed as  $-K_{II}^{-1} K_{IB}$ ,  $X_{el}$  is the matrix of fixed interface modes, i.e. the matrix of the eigenvectors of  $(K_{II}, M_{II})$ , and  $\alpha$  is the vector of the modal amplitudes.

To reduce the size of the problem, only a limited number of fixed interface modes of amplitudes  $\tilde{\alpha}$  is retained. The internal DOFs are then approximated by

$$\{\tilde{q}_I\} \approx [X_{st}]\{q_B\} + [\tilde{X}_{el}]\{\tilde{\alpha}\} \quad (4)$$

where  $\tilde{X}_{el}$  is a matrix of reduced size. Inserting Eqs. (3) and (4) into Eq. (2) leads to a system of reduced size easier to invert.

## 3 Sparse Polynomial Chaos

### 3.1 Generalized polynomial chaos

The generalized polynomial chaos (gPC) has been proposed by Xiu and Karniadakis [10]. It consists in expanding a random process  $X(\xi)$  depending on  $r$  independent random variables  $(\xi_1, \dots, \xi_r) = \xi$  as follows:

$$X(\xi) = \sum_{\alpha \in \mathbb{N}^r} \bar{x}_\alpha \phi_\alpha(\xi), \quad (5)$$

where  $\phi_\alpha(\xi)$  are orthogonal polynomials which represent the stochastic components of the process, and  $\bar{x}_\alpha$  are the PC coefficients that account for the deterministic components of the process.

The Wiener theory as well as the generalized Cameron-Martin theorem [11] state that the series is convergent in the mean square sense. According to the Askey scheme, if  $\xi$  is a uniform random vector, the polynomial functions  $\phi_\alpha$  are most suitably obtained from Legendre polynomials [12, 10, 13].

In practice, the random process  $X(\xi)$ , which constitutes the quantity of interest (QoI), is approached by a truncated expansion as

$$X(\xi) \approx \sum_{\alpha \in \mathcal{A}^{r,p}} \bar{x}_\alpha \phi_\alpha(\xi), \quad (6)$$

where  $p$  is the order of the PC expansion and  $\alpha = \{\alpha_1, \dots, \alpha_r\} \in \mathbb{N}^r$ . The index set used in the truncated expansion (6) is then defined as

$$\mathcal{A}^{r,p} = \{\alpha \in \mathbb{N}^r : \|\alpha\|_1 \leq p\}, \quad (7)$$

with

$$\|\alpha\|_1 = \sum_{i=1}^r \alpha_i. \quad (8)$$

Computing the QoI  $X$  comes down to finding the coefficients  $\bar{x}_\alpha$  of the truncated gPC expansion Eq. (6). The number of terms  $N_p$  is linked to the order  $p$  and to the number of uncertain parameters  $r$  as [10]

$$N_p = \text{card}(\mathcal{A}^{r,p}) = \frac{(p+r)!}{p!r!}. \quad (9)$$

In this study, the QoIs are quantities such as a displacement or an energy quantity that are solutions of a FE model. The PC coefficients are here determined from a non-intrusive regression method that does not require any modification of the FE model: they are built from a finite number  $Q = k N_p$  (with  $k$  a small integer usually equal to 2, 3 or 4) of values of the QoI  $X$ , computed from numerical  $Q$  simulations of the FE model. In practice the  $Q$  sets of values of the uncertain parameters for which the QoI is computed, which will be referred to as the nested experimental design (NED) in the following, may be chosen with a Latin Hypercube Samples (LHS) method [14].

Within the regression framework, the evaluation of the coefficients results from the minimization of the following criterion [15]

$$\varepsilon_{reg}^2 = \sum_{q=1}^Q \left[ X(\xi^{(q)}) - \sum_{\alpha \in \mathcal{A}^{r,p}} \bar{x}_\alpha \phi_\alpha(\xi^{(q)}) \right]^2, \quad (10)$$

where  $\xi^{(q)} = (\xi_1^{(q)}, \dots, \xi_r^{(q)})$  (with  $q = 1, \dots, Q$ ) denotes the Numerical Experimental Design (NED), that is the set of  $Q$  vectors of uncertain parameter values generated from the probabilistic support of the parameters;  $X(\xi^{(q)})$  denotes the vector of the corresponding FE model evaluations. The PC coefficients are finally calculated as

$$\bar{x} = \left( \phi^T(\xi^{(q)}) \phi(\xi^{(q)}) \right)^{-1} \phi^T(\xi^{(q)}) X(\xi^{(q)}), \quad (11)$$

with  $\phi(\xi^{(q)})$  the matrix defined by

$$\phi(\xi^{(q)}) = \begin{pmatrix} \phi_0(\xi^{(1)}) & \dots & \phi_{N_p-1}(\xi^{(1)}) \\ \vdots & \ddots & \vdots \\ \phi_0(\xi^{(Q)}) & \dots & \phi_{N_p-1}(\xi^{(Q)}) \end{pmatrix}. \quad (12)$$

If the number of uncertain parameters and the order  $p$  of the gPC expansion are high, the number of PC coefficients and therefore the necessary number of simulations to build them become quickly prohibitive. Strategies to reduce this number of simulations are consequently necessary.

### 3.2 Sparse Polynomial Chaos

The sparse Polynomial Chaos (sPC) can reduce the number of PC coefficients. In this paper, sPC with anisotropic hyperbolic index sets will be used.

### 3.2.1 Anisotropic hyperbolic index sets

The strategy to truncate the PC expansions favors input random variables  $\xi_i$  with large total sensitivity indices  $S_i^T$ . For this purpose, the truncation is based on the following anisotropic norm

$$\|\alpha\|_{m,w} = \left( \sum_{i=1}^r |w_i \alpha_i|^m \right)^{1/m}, \quad w_i \geq 1. \quad (13)$$

The corresponding anisotropic index set is then chosen as

$$\mathcal{A}_{m,w}^{r,p} = \{\alpha \in \mathbb{N}^r : \|\alpha\|_{m,w} \leq p\}, \quad (14)$$

where  $w$  is a set of weights  $w_i$  defined by

$$w_i = 1 + \frac{\max_{1 \leq j \leq r} S_j^T - S_i^T}{\sum_{k=1}^r S_k^T}. \quad i = 1, \dots, r. \quad (15)$$

In the above equation,  $S_i^T$  is the PC-based total sensitivity index [16] of the QoI with respect to the input random variable  $\xi_i$ , and is computed as

$$S_i^T = \frac{1}{D_{PC}} \sum_{\alpha \in \mathcal{I}_i^+} \bar{x}_\alpha^2 \mathbb{E}[\phi_\alpha^2(\xi)], \quad (16)$$

where  $\mathcal{I}_i^+$  denotes the set of indices having a non-zero  $i^{\text{th}}$  component

$$\mathcal{I}_i^+ = \{\alpha \in \mathcal{A}_{m,w}^{r,p} : \alpha_i \neq 0\}, \quad (17)$$

and  $D_{PC}$  the variance of the QoI

$$D_{PC} = \sum_{\alpha \in \mathcal{A}_{m,w}^{r,p}} \bar{x}_\alpha^2 \mathbb{E}[\phi_\alpha^2(\xi)]. \quad (18)$$

The anisotropic hyperbolic polynomial chaos expansions are finally defined with the index sets  $\mathcal{A}_{m,w}^{r,p}$  as

$$X_{\mathcal{A}_{m,w}^{r,p}}(\xi) = \sum_{\alpha \in \mathcal{A}_{m,w}^{r,p}} \bar{x}_\alpha \phi_\alpha(\xi). \quad (19)$$

### 3.2.2 Error estimates of the polynomial chaos approximations

The building of a sparse PC expansion is based on an iterative search of the significant PC coefficients, and therefore requires the use of error estimates to assess the accuracies of the consecutive PC approximations.

A relevant theoretical error in this context is defined as follows:

$$Err = \mathbb{E}[(X(\xi) - \widehat{X}_{\mathcal{A}}(\xi))^2], \quad (20)$$

which is based on the difference between the deterministic evaluation  $X(\xi)$  of the QoI and its PC approximation  $\widehat{X}_{\mathcal{A}}(\xi)$  computed from a finite non empty subset  $\mathcal{A} \subset \mathbb{N}^r$ , that is

$$\widehat{X}_{\mathcal{A}}(\xi) = \sum_{\alpha \in \mathcal{A}} \bar{x}_\alpha \phi_\alpha(\xi). \quad (21)$$

The generalization error is estimated in practice by the following empirical error:

$$Err_{emp} = \frac{1}{Q} \sum_{q=1}^Q \left[ (X(\xi^{(q)}) - \widehat{X}_{\mathcal{A}}(\xi^{(q)}))^2 \right] \quad (22)$$

in which the differences are computed specifically at the  $Q$  observations of a NED  $\xi^{(q)} = (\xi_1^{(q)}, \dots, \xi_r^{(q)})$ . The latter will be used in the following to compute a coefficient of determination  $R^2$  defined as

$$R^2 = 1 - \frac{Err_{emp}}{\widehat{V}[X]}, \quad (23)$$

where  $\widehat{V}[X]$  is the variance of  $X(\xi^{(q)})$ :

$$\widehat{V}[X] = \frac{1}{Q-1} \sum_{q=1}^Q (X(\xi^{(q)}) - \bar{X})^2 \quad \text{with} \quad \bar{X} = \frac{1}{Q} \sum_{q=1}^Q X(\xi^{(q)}).$$

An overfitting phenomenon is likely to occur when using the empirical error, which, as a consequence, underestimates the generalization error. The leave-one-out error [17], which is based on a sum of squared predicted residuals  $\Delta^{(i)}$  defined hereafter, may be useful to avoid this drawback. A predicted residual expresses the difference between the deterministic evaluation  $X(\xi^{(i)})$  of the QoI at the  $i^{\text{th}}$  observation of the NED  $\xi^{(q)}$ , and its prediction  $\widehat{X}_{\mathcal{A}}^{(-i)}(\xi^{(i)})$  obtained with a PC expansion  $\widehat{X}_{\mathcal{A}}^{(-i)}$  built from a reduced NED  $(\xi^{(1)}, \dots, \xi^{(Q)}) \setminus \xi^{(i)}$  (that is the original NED from which the observation  $\xi^{(i)}$  has been discarded) [7]:

$$\Delta^{(i)} = X(\xi^{(i)}) - \widehat{X}_{\mathcal{A}}^{(-i)}(\xi^{(i)}). \quad (24)$$

The leave-one-out error is then defined as

$$Err_{LOO} = \frac{1}{Q} \sum_{i=1}^Q (\Delta^{(i)})^2. \quad (25)$$

In practice, the predicted residual  $\Delta^{(i)}$  may be computed as [17]

$$\Delta^{(i)} = \frac{X(\xi^{(i)}) - \widehat{X}_{\mathcal{A}}(\xi^{(i)})}{1 - h_i}, \quad (26)$$

where  $h_i$  is the  $i^{\text{th}}$  diagonal term of the matrix  $\phi(\xi^{(q)}) (\phi^T(\xi^{(q)}) \phi(\xi^{(q)}))^{-1} \phi^T(\xi^{(q)})$ . The leave-one-out error is in that case given by

$$Err_{LOO} = \frac{1}{Q} \sum_{i=1}^Q \left( \frac{X(\xi^{(i)}) - \widehat{X}_{\mathcal{A}}(\xi^{(i)})}{1 - h_i} \right)^2. \quad (27)$$

A determination coefficient  $S^2$  equivalent to that of the empirical error,  $R^2$ , may be defined for the leave-one-out error:

$$S^2 = 1 - \frac{Err_{LOO}}{\widehat{V}[X]}. \quad (28)$$

The two coefficients  $R^2$  and  $S^2$  defined above will be used in an algorithm whose aim is to build an optimal sparse PC expansion involving the most significant terms from an adapted NED of reduced size. This algorithm is described in the next section.

### 3.2.3 sPC expansion building algorithm

As explained previously, the efficiency of the method may be increased by retaining only the most significant PC polynomials [7] among those corresponding to the index sets  $\mathcal{A}_{m,w}^{r,p}$ . In the following, the final index sets of the kept terms are denoted as  $\mathcal{A}_{m,w}^p$ .

The search for those most significant coefficients is performed through an iterative procedure which is summarized below in 5 basic steps.

#### Step 1

Select a NED  $(\xi^{(q)})$ , e.g. a random design based on LHS [14], of arbitrary size  $Q_k = 4N_p$ , where  $N_p$  is determined by Eq. (9) with  $r$  uncertain parameters and  $p = 1$ . The FE model evaluations at the NED points are gathered in the vector  $X(\xi^{(q)})$ . Set arbitrarily the values of the parameters corresponding to the chosen sparse PC method: the maximal PC order  $p_{max}$  and the coefficient  $m$  used for the  $m$ -norm of truncation, as well as the target accuracy  $S_{target}^2$  and two thresholds  $\epsilon_1$  and  $\epsilon_2$ .

#### Step 2

Initialize the algorithm: the PC order is set to  $p = 0$ , and the truncation index set to the null element of  $\mathbb{N}^r$ ,  $\{0\}$ ; the vector of weights  $w_i$  is set to  $w = \{1, \dots, 1\}$ . The corresponding initial values of the determination coefficients are denoted as  $R_0^2$  and  $S_0^2$ .

#### Step 3: Training step - Enrichment of the PC basis

Increment the order value:  $p \rightarrow p + 1 \in [1, \dots, p_{max}]$ .

⇒ **Forward step** (Addition step): For each term from the candidate set  $\{\alpha \in \mathbb{N}^r : p - 1 \leq \|\alpha\|_{m,w} \leq p\}$ , add it to the set  $\mathcal{A}_{m,w}^{p-1}$  and compute, as above, the PC coefficients and the determination coefficient  $R^2$ . Retain only terms which lead to a significant increase in the value of the coefficient  $R^2$ , i.e.  $\Delta R^2 = R^2 - R_0^2 \geq \epsilon_1$ . Let  $\mathcal{A}_{m,w}^{p+}$  be the final truncation set at this stage.

⇒ **Backward step** (Elimination step): Remove in turn each term in  $\mathcal{A}_{m,w}^{p+}$  of order strictly lower than  $p$ , and compute again the PC expansion coefficients and the associated coefficient  $R^2$  in each case. Discard from  $\mathcal{A}_{m,w}^{p+}$  the terms that lead to an insignificant decrease in  $R^2$ , i.e.  $\Delta R^2 = R_0^2 - R^2 < \epsilon_2$ . Let  $\mathcal{A}_{m,w}^p$  be the final truncation set. The total sensitivity indices  $S_i^T$  of the current PC approximation are computed and the weights  $w_i$  are updated (Eq. (15)).

#### Step 4: Verification of the conditioning of the regression information matrix

If the conditioning is satisfying, i.e. the size  $Q_k$  of the NED ( $\xi^{(q)}$ ) is larger than  $2 \cdot \text{card}(\mathcal{A}_{m,w}^p)$  go to step 5. If the conditioning is poor, i.e. the size  $Q_k$  of the NED ( $\xi^{(q)}$ ) is smaller than  $2 \cdot \text{card}(\mathcal{A}_{m,w}^p)$ , an enrichment of the NED is done using nested Latin Hypercube designs [18, 7] to reach a size  $Q_{k+1}$ . In this case, the truncation set is reset to  $\{0\}$  and the enrichment procedure is restarted from step 2.

#### Step 5: Test step

Stop if either the leave-one-out error  $S_0^2$  is larger than the target value  $S_{target}^2$  or if the order of the PC expansion is equal to  $p_{max}$ . Otherwise, go back to step 3.

The detailed algorithms are presented in Figure 1.

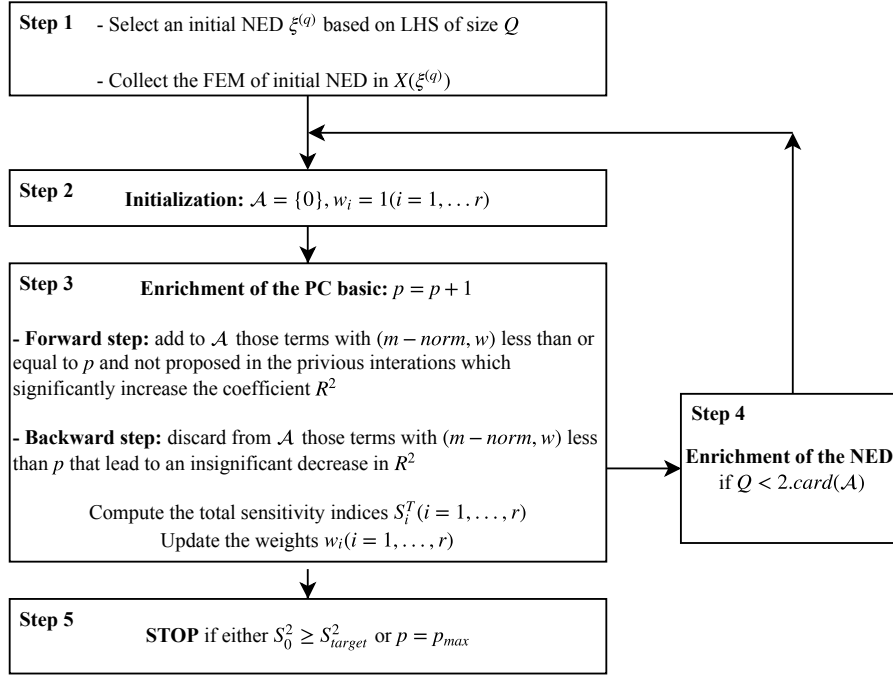


Figure 1: Algorithm applied to build a sparse polynomial chaos expansion with anisotropic hyperbolic index sets

## 4 Results

### 4.1 Application model of three plates connected by springs with uncertain stiffness

The method is applied to a system composed of three plates connected together through torsional and translational lineic springs as shown in Figure 2. Plates 1 and 3 are identical  $1 m \times 1 m$  square plates made of steel, with the following material properties: density  $\rho = 7850 kg/m^3$ , Young's modulus  $E = 2 \times 10^{11} Pa$  and Poisson's ratio  $\nu = 0.3$ . The remaining plate 2, of dimensions  $0.2 m \times 1 m$ , represents a soft junction made up of rubber; the corresponding material properties are chosen as  $\rho = 950 kg/m^3$ ,  $E = 15 \times 10^7 N/m^2$  and  $\nu = 0.48$ . Within the FE framework, the three plates of same thickness  $5 mm$  are meshed using square plate elements of

length  $0.025\text{ m}$  having three DOFs per node, namely the displacement  $u_z$  and two rotations  $\theta_x, \theta_y$ . The meshes of plates 1 and 3 therefore involves 1600 elements and 5043 DOFs, while 320 elements and 1107 DOFs are used for plate 2.

The torsional stiffness of the springs along the  $x$ - and  $y$ - directions is assumed to be uniform and equal to  $20\text{ Nm/rad}$ , whereas in the  $z$ -direction the stiffness  $k_z$  is supposed to represent a random variable following a uniform probability law over the range  $[100, 200]\text{ N/m}$ . The whole structure is clamped at both extremities (i.e., left edge of plate 1 and right edge of plate 3) and subjected to a harmonic point force of amplitude  $F = 40\text{ N}$  in the  $z$ -direction, located at the node of coordinates  $(0.25\text{ m}, 0.25\text{ m})$  if the origin is chosen as the lower left corner of plate 1.

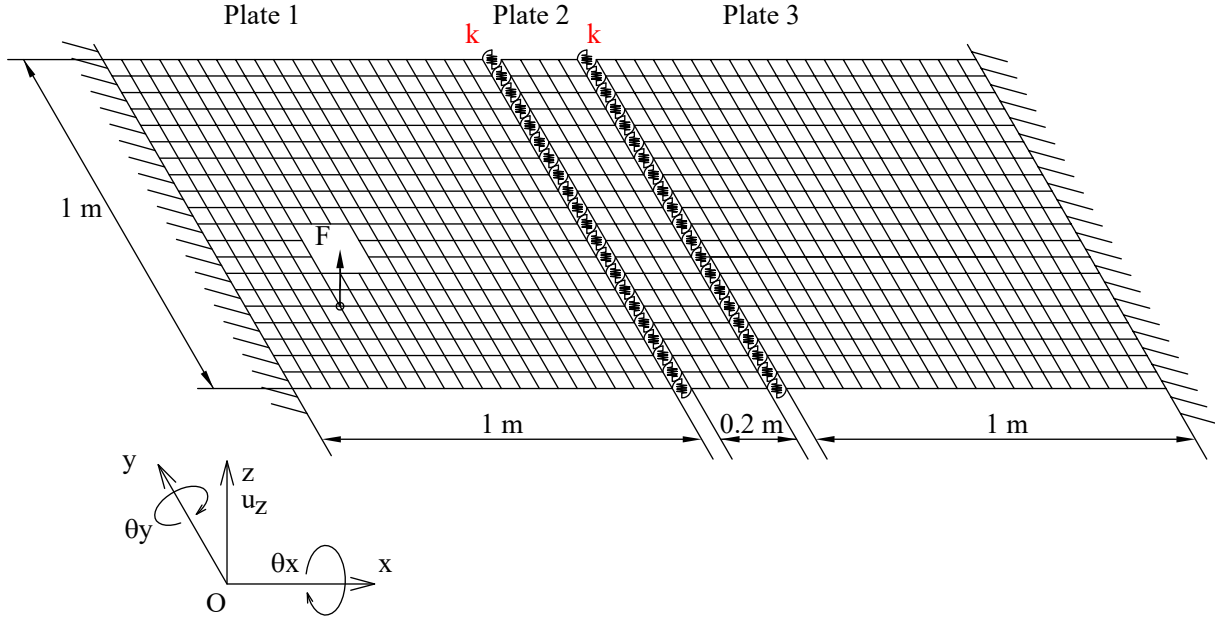


Figure 2: Model of three plates connected by springs

The frequency response function of the structure is studied within the frequency band  $[0, 50]\text{ Hz}$  using a frequency step of  $10^{-3}\text{ Hz}$ . Examples of FRFs are provided in Figure 3, which represents the frequency evolutions of the deformation energy of plate 1,  $E_{def1}$ , for three values of the spring stiffness  $k_z$  (namely the two extreme values  $100\text{ N/m}$  and  $200\text{ N/m}$ , and the nominal value  $150\text{ N/m}$ ). As it can be seen in Figure 3, the curves present a similar trend with extrema at the resonance frequencies of the system, but the amplitudes and the frequencies of those peaks depend on the value of the stiffness  $k_z$ .

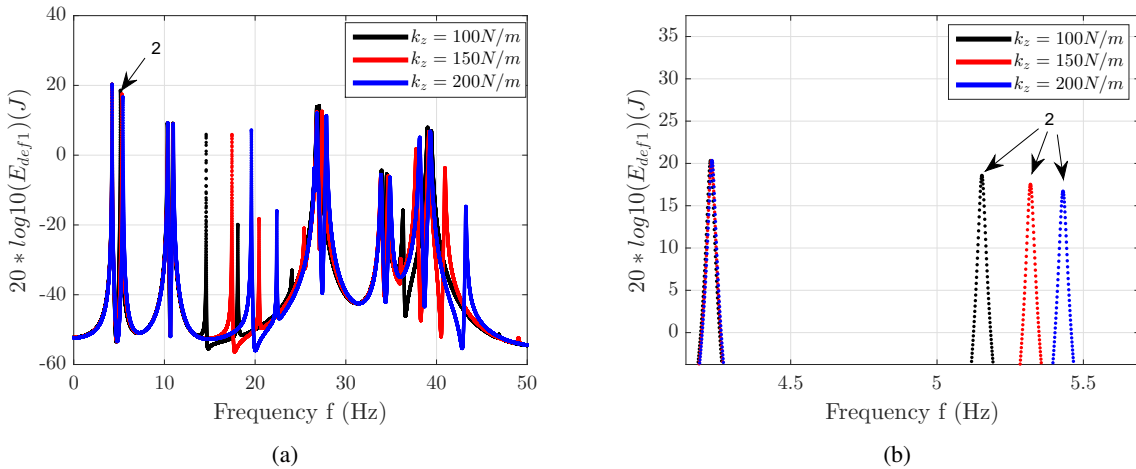


Figure 3: Deformation energy  $E_{def1}$  of plate 1: (a) whole frequency range (b) zoom on the first two peaks



## 4.2 Quantities of interest and statistics

In the following, we will focus on two particular QoIs related to the second peak visible on the  $E_{def1}$  curves, which is displayed in a detailed view in Figure 3(b): the frequency and the amplitude of the peak. Both QoIs are determined from a maximum search over a small frequency band around the frequency of the peak obtained at the nominal value of  $k_z$ .

The statistics (e.g. mean value and variance) of each QoI are computed within a Monte-Carlo procedure involving a number  $N$  of simulations that correspond to  $N$  values of  $k_z$  chosen uniformly within the range  $[100, 200]N/m$ . Those  $N$  simulations may involve:

- the initial FEM model, which involves a total number of 11193 DOFs; the statistics obtained with this model will be considered as the reference solution in the following;
- a reduced model resulting from a Craig-Bampton decomposition in which a limited number of fixed interface modes is retained; two CB models will be proposed in the following: the first one, denoted as CB50130, involves 50 fixed interface modes for plates 1 and 3 (out of 4563 modes), and 130 modes for plate 2 (out of 819 modes); in the second one, denoted as CB3080, 30 modes are retained for plates 1 and 3 and 80 for plate 2;
- the sPC expansion of the QoI in which the coefficients have been built from a limited number of simulations using the initial FE model, denoted as sPC-FEM;
- an sPC expansion whose coefficients are built from simulations involving one of the two aforementioned reduced CB models, denoted respectively as sPC-CB50130 and sPC-CB3080.

For each QoI, comparisons between the statistics computed from the first three models will provide information on the direct influence of the CB reduction on the accuracy of the results with respect to the full initial FE model. At a second level, comparisons between the results from the FEM and sPC-FEM methods will give insight into the influence of the use of a sparse PC expansion on the accuracy of the statistics. Finally, the influence of the model reduction on the sPC expansions will be studied through the last sPC-CB50130 and sPC-CB3080 methods.

In the following, the results related to the first QoI, namely the resonance frequency of the second peak of the deformation energy  $E_{def1}$ , are first gathered in section 4.3. The results related to the amplitude of the peak are then presented in section 4.4.

## 4.3 $E_{def1}$ peak 2 resonance frequency

### 4.3.1 Building of the sPC expansions

The different sPC expansions of the two QoIs are built in accordance with the iterative procedure detailed in section 3.2.3. The same set of parameters is used in all the cases: the maximal PC order is set to  $p_{max} = 6$ , the target accuracy is chosen as  $S_{target}^2 = 0.999$ , and we use two identical thresholds  $\epsilon_1 = \epsilon_2 = 0.001(1 - S_{target}^2)$ .

As explained previously, the optimal order  $p$  of the sPC expansion of the QoI depends on the leave-one-out error  $S_0^2$  that is computed at each step of the iterative procedure and compared to the target accuracy  $S_{target}^2$ . For the first QoI (peak 2 resonance frequency), the values of  $S_0^2$  obtained for the three sPC expansions (sPC-FEM, sPC-CB50130 and sPC-3080) are  $S_0^2 = 0.9820$  for  $p = 1$  and  $S_0^2 = 0.9997$  for  $p = 2$ . The optimal order for the three sPC expansions is therefore  $p = 2$ .

### 4.3.2 Accuracy of the QoI statistics obtained from the different methods

The statistics (mean and variance) of the QoI depend on the number of simulations  $N$  chosen within the MC procedure. Several tests ranging from  $N = 1000$  to  $N = 10000$  have been performed for each of the six methods detailed in the previous section. Figure 4 compares the statistics obtained with the six strategies detailed in the previous section for ten values of  $N$  ranging from  $N = 1000$  to  $N = 10000$ . The mean value and the variance of the frequency are seen to reach a stabilized value from  $N = 2000$ . Two groups of curves are visible on each graph, meaning that the use of an sPC expansion (whatever the model chosen to build the PC coefficients)

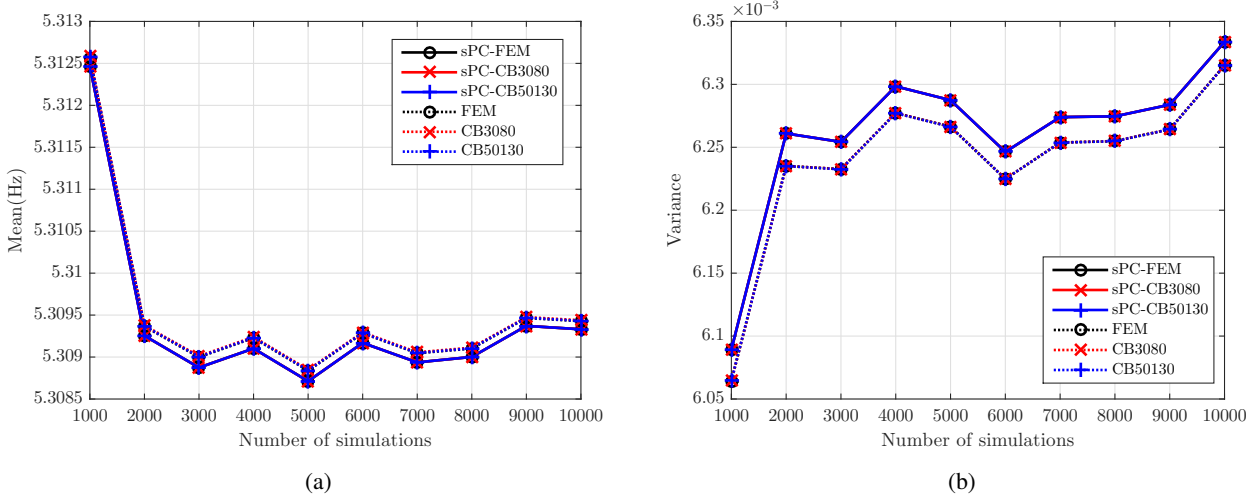


Figure 4: (a) Mean and (b) variance of the QoI according to the number of MC simulations

induces a slight change in the resulting mean and variance values; the use of a model reduction does not modify the statistics significantly.

The low variance levels obtained in Figure 4(b) also reduce the confidence intervals relative to the mean resonance frequency. For instance, for  $N = 10000$ , the mean resonance frequency of peak 2 lies in the interval  $\bar{f}_2 \pm 1.2 \cdot 10^{-4}$  with a confidence level of 95 %.

To further analyze the accuracies of the different method, the relative errors of the mean value of the QoI and its variance with respect to the reference solution (i.e.  $N$  simulations from the initial FE model) are displayed in Figure 5. The lowest error levels are logically obtained with the CB50130 method, which involves  $N$  direct simulations with the reduced CB model with the largest basis of fixed interface modes. Further reducing the size of the mode basis slightly increases the error levels, but the accuracy remains in both cases excellent, with error levels close to 0. The use of an sPC expansion increases the error levels, which remain however lower than  $2.5 \cdot 10^{-3} \%$  for the mean value and 0.5 % for the variance. Choosing a reduced model instead of the original FE model to compute the coefficients of the sPC does not increase the error levels for this QoI.

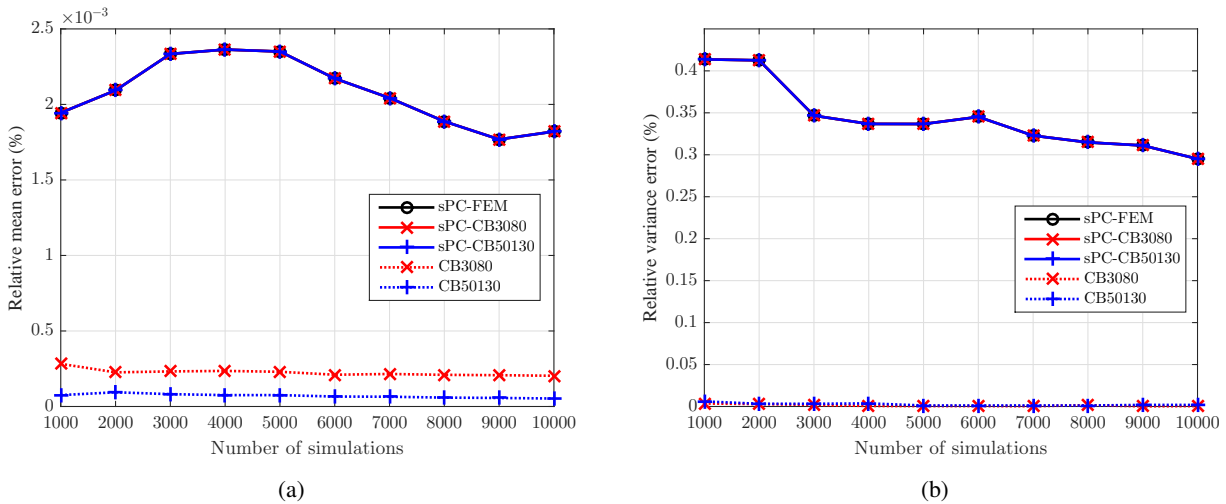


Figure 5: Relative errors of (a) the mean value of the QoI and (b) the variance of the QoI with respect to the reference solution according to the number of MC simulations

Same conclusions arise when studying the mean (Figure 6(a)) and maximum (Figure 6(b)) values of the relative errors of the QoI for a given  $N$  number of simulations (i.e. a relative error is computed for each of the  $Nk_z$  values between the peak 2 frequency obtained with the considered method and the frequency found using the initial FE model; the mean value is then computed over the  $k_z$  range  $[100, 200]N/m$ , along with the maximum value). The errors mainly come from the sPC expansions, the influence of the model reduction being again very limited; the accuracy level is also extremely satisfying with a mean relative error lower than 0.015 %

and maximum error lower than 0.05 % whatever the retained  $N$  number of simulations.

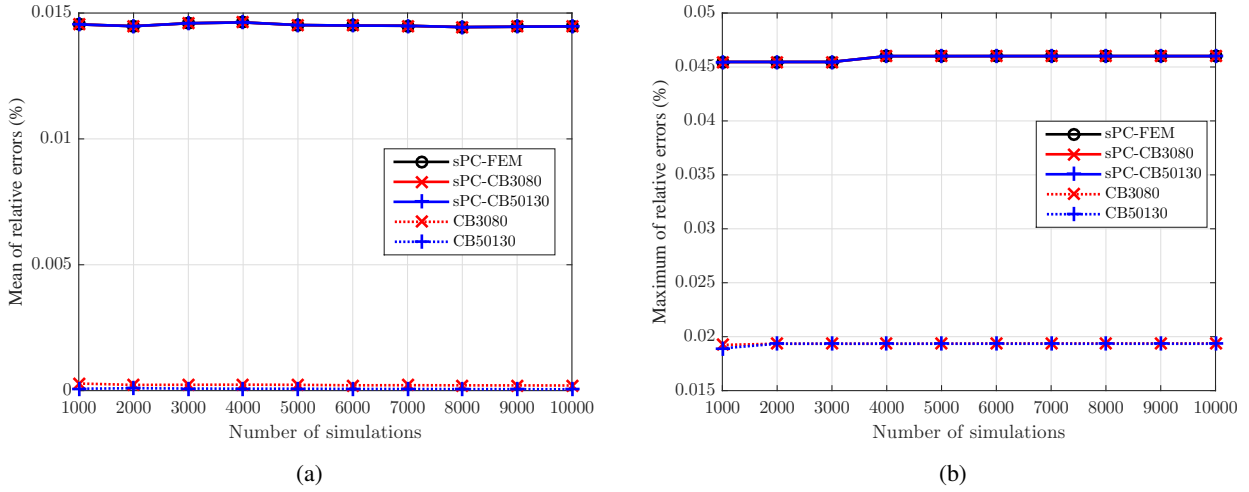


Figure 6: (a) Mean and (b) maximum values of the relative errors of the QoI with respect to the reference solution according to the number of simulations

### 4.3.3 Evolutions of the resonance frequency according to $k_z$

The results in this section are presented for the highest number  $N = 10000$  of simulations, to ensure that the QoI is predicted with the highest confidence level. Figure 10 represents the values of the second resonance frequency obtained for each of the 10000  $k_z$  values chosen within the range  $[100, 200] N/m$  with the different methods: direct simulations with the initial FE model or the reduced ones, or estimations from the three sPC expansions. The QoI exhibits a non linear increasing dependency to the stiffness  $k_z$ , with a global variation of about 5 % with respect to its mean value. An overall good agreement is found between the different strategies, as the six curves appear superimposed of the whole  $k_z$  range (Figure 10(a)). However, when zooming on a smaller range of  $k_z$  values, such as in Figure 10(b), the slight differences behind the error levels presented previously become visible. The curves corresponding to the three methods that involve direct FE simulations (FEM, CB50130 and CB3080) present discontinuities that are linked to the frequency step used in this study, 0.001 Hz; the peak frequency is either underestimated or overestimated according to the  $k_z$  value as its precision cannot exceed the frequency resolution of the simulations. Predicting the frequency value from an sPC expansion avoids this behavior, as the frequency becomes a polynomial function of  $k_z$ . The curves corresponding to the three sPC expansions are therefore continuous plots that can be hardly distinguished from one another.

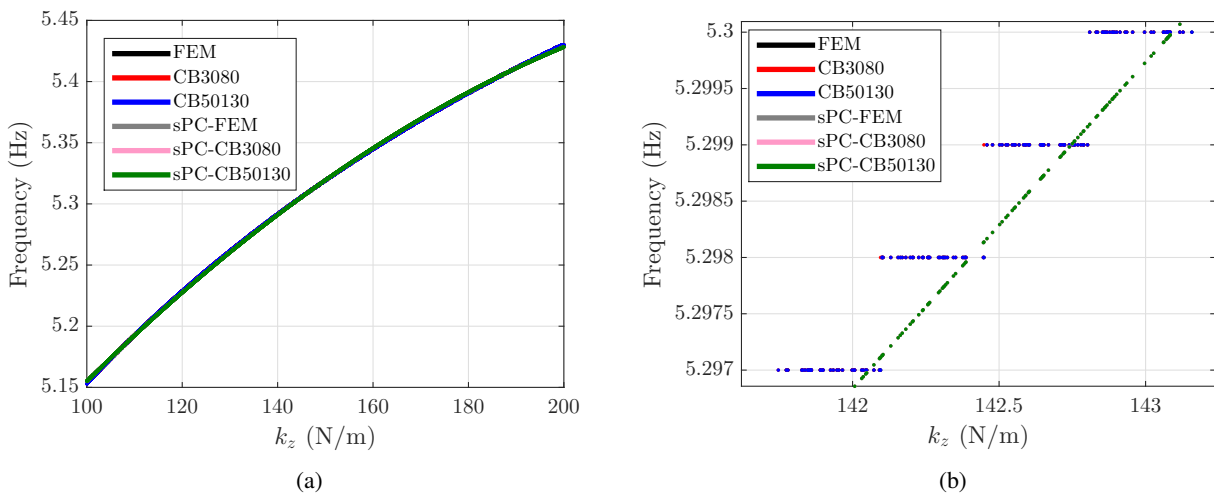


Figure 7: Peak 2 resonance frequency according to the spring stiffness  $k_z$  for  $N = 10000$

## 4.4 Amplitude of the deformation energy peak 2

### 4.4.1 Building of the sPC expansions

The sPC expansions of the second QoI are built using the same parameters and iterative procedure as the resonance frequency. Leave-one-out error  $S_0^2$  is used to choose the optimal order  $p$  of the polynomial chaos to calculate QoI that is  $E_{def1}$  in this section. The leave-one-out errors  $S_0^2$  for the second QoI are similar for  $p = 1$  and  $p = 2$  to those obtained for the frequency, the optimal PC order being again  $p = 2$ .

### 4.4.2 Accuracy of the QoI statistics

As for the resonance frequency, the statistics related to the amplitude of the deformation energy at the second peak are computed from  $N$  simulations corresponding to  $N$  values of  $k_z$ , from  $N = 1000$  to  $N = 10000$ . The same trends as for the first QoI are retrieved, that will be illustrated hereafter for the variance only.

Figure 8(a) displays the variance of the QoI with respect to the number of simulations  $N$ , a stabilized value being again reached from  $N = 2000$ . As for the first QoI (frequency), two groups of curves emerge from the figure, which correspond respectively to the simulations involving the initial or reduced FE models, and to those based on the sPC expansions. The relative errors between the variance values with respect to the reference solution are shown in Figure 8(b), and exhibit overall very satisfying levels although they are higher than those obtained for the the resonance frequency. The use of a reduced basis instead of the initial FE model has again little impact in terms of variance errors, as the highest level error, corresponding to the CB3080 method, is about 0.02%. The influence of the sPC expansions on the accuracy of the variance estimation is more important, as they induce error levels of about 1%. The best results are obtained when the sPC coefficients are computed using the initial FE model (sPC-FEM case) while the error levels increase up to 1,1% with the sPC-CB3080 methods.

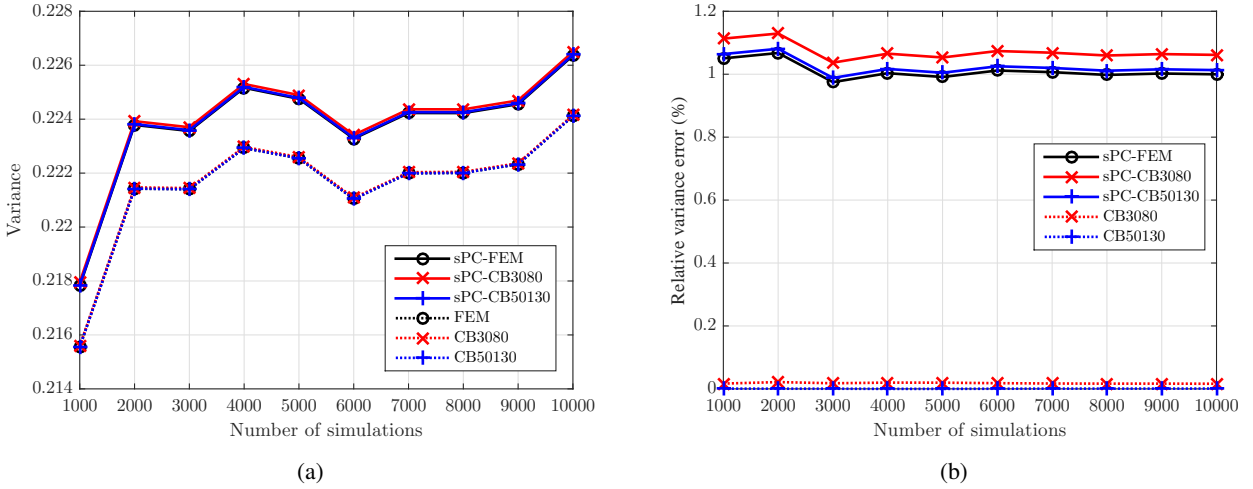


Figure 8: (a) Variance and (b) relative error of the variance of the second QoI according to the number of MC simulations

Figure 9 displays the mean and maximum error levels attained when computing the relative errors, for each  $k_z$  value, between the peak 2 amplitudes resulting of a given method (involving a reduced basis or an sPC expansion) and those obtained with the reference solution (involving the initial FE model). As previously, the error levels are constant from  $N = 2000$  and result mainly from the use of an sPC expansion, while the CB reduction induces low additional errors. All the methods provide an excellent accuracy with overall very low error levels. For instance, the mean error level is about 0.002% with the CB50130 method, 0.01% with the CB3080 method and 0.065% with any of the sPC expansions. The maximum error values are of the same order of magnitude, from 0.005% and 0.02% with the reduced models (CB50130 and CB3080 respectively) to 0.2% with the sPC expansions, the highest value being obtained when the sPC coefficients are computed using the CB2080 model.

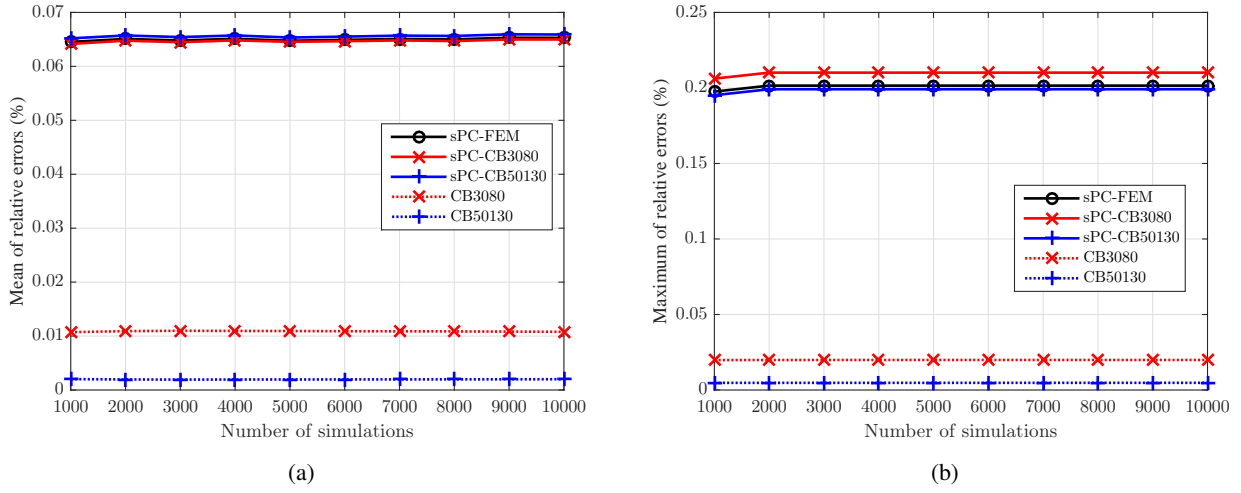


Figure 9: (a) Mean and (b) maximum values of the relative errors of the QoI with respect to the reference solution according to the number of simulations

#### 4.4.3 Evolutions of the amplitude of peak 2 according to $k_z$

The evolutions of the amplitude of the second resonance peak of  $E_{def1}$ , directly computed with  $N = 10000$  simulations of the initial FE model or a reduced CB model, or predicted by one of the three sPC expansions, are finally plotted in Figure 10. The QoI is here a decreasing non linear function of the stiffness  $k_z$ , and the six curves appear again superimposed throughout the whole  $k_z$  range. The discrepancies between the solutions are revealed in the detailed view (Figure 10(b)), where two groups of curves are again visible. The first group gathers the simulations involving direct FE simulations, for which the frequency of peak 2 could be under- or overestimated due to the limited frequency step of  $0.001 \text{ Hz}$  (cf. Figure 10(b)). These approximations in the resonance frequency values lead to an underestimation of the peak amplitude and results in the uneven appearances of the curves. The latter reach their maximum values when the peak resonance frequency value coincides with a multiple value of the frequency step. The use of an sPC expansion to predict the peak amplitude appears again efficient to solve this issue, as the resulting curves are smooth and match the maximum values of the first group.

Regarding the accuracy of the predictions, it can be seen that within the first group, the CB50130 is perfectly superimposed with the reference FEM curve, while the CB3080 is slightly shifted (but remains very close to the first two curves). This trend is retrieved in the second group, where the curve corresponding to the sPC-CB3080 does not perfectly superimpose with the two other curves, although the differences are extremely weak.

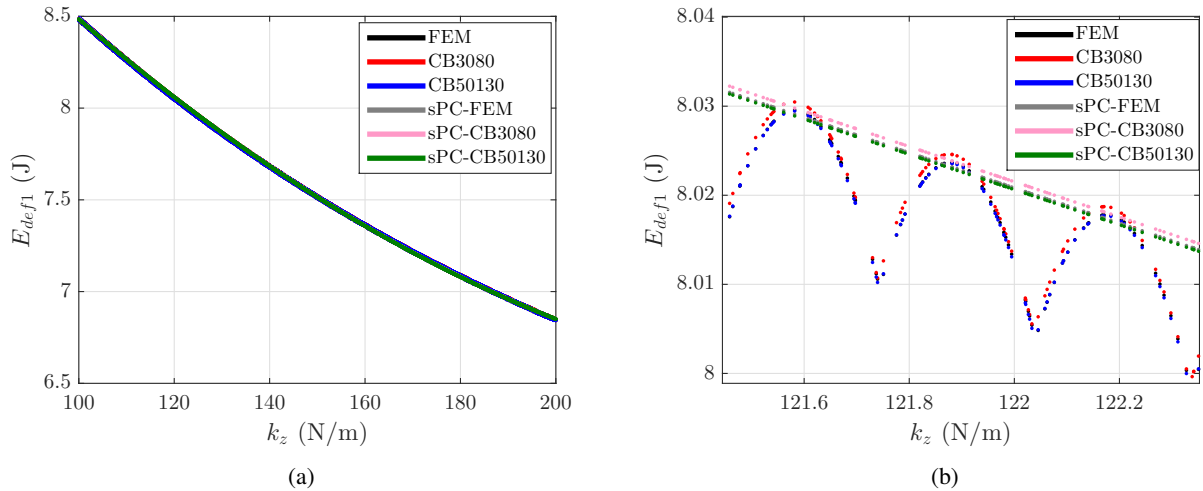


Figure 10: Peak 2 amplitude according to the spring stiffness  $k_z$  for  $N = 10000$

## 4.5 Computational costs

The previous results have clearly established that an sPC expansion was efficient to produce accurate predictions of the different QoIs evolutions with respect to the uncertain parameter (i.e. the spring stiffness  $k_z$ ). The main interest of the method is that the computational costs are also extremely decreased due to the limited number of simulations necessary to compute the sPC coefficients. To illustrate this benefit, the computational costs per QoI related to the six aforementioned methods are presented in table 1 for  $N = 10000$ . The reference solution is obviously the most expensive as it implies  $N = 10000$  simulations with the FE model owning the highest number of DOFs. Substantial cost reductions are already achieved when using a FE model of reduced size instead of the original model to perform those 10000 simulations. With the most reduced basis (CB3080), the computational time reduction reaches 73.16% without loss of accuracy. The advantage of the sPC expansions is that the number of simulations necessary to compute the PC coefficients is very limited. Applying the iterative procedure depicted previously, we obtain the coefficients for  $p = 2$  and one uncertain parameters with only 14 simulations. Once the coefficients are known, performing 100000 computations to calculate the QoI is costless. The computational time reduction therefore exceeds 99% for the three proposed sPC expansions. The highest reduction (99.96%) is logically obtained when the coefficients are computed using the most reduced CB3080 model.

Method	FEM	CB50130	CB3080	sPC-FEM	sPC-CB50130	sPC-CB3080
Computational time formula	Nb of FEM x Unit time per full FEM	Nb of reduced FEM x Unit time per reduced FEM	Nb of reduced FEM x Unit time per reduced FEM	Nb of FEM to build chaos x Unit time per full FEM	Nb of reduced FEM to build chaos x Unit time per reduced FEM	Nb of reduced FEM to build chaos x Unit time per reduced FEM
Nb of simulations with full or reduced FEM	10000	10000	10000	14	14	14
Computational time	15 days 20h	5 day 6h	6 days 6h	32 min	11 min	9 min
Computational time reduction (%)	-	66.84	73.16	99.86	99.95	99.96

Table 1: Computational costs for one QoI and  $N = 10000$  with the different methods

## 5 Conclusion

In this paper, we have proposed a strategy to analyze the dynamic response of a structure having a large number of DOFs and uncertain parameters in the FE framework. The retained method associates the use of a sparse PC expansion to compute the quantities of interest (e.g. a displacement or a energy quantity such as a deformation energy) and a model reduction based on the Craig-Bampton decomposition to obtain at low cost the PC coefficients.

This strategy has been successfully applied to the case of a structure, composed of several plates connected with springs, presenting one uncertain parameter, namely the spring stiffness  $k_z$ . The CB reduction has shown to produce a negligible loss of accuracy while ensuring a substantial reduction of the computational cost. Combining the use of such a reduced model with an sPC expansion, the accuracy of the results remains fully satisfying and the computational time reduction reaches exceptional levels.

In a near future, the proposed strategy will be applied to complex systems characterized by a larger number of uncertain parameters. The benefits of using a sparse PC expansion instead of the classic generalized PC expansion will then become more evident, as the computational cost necessary to compute the PC coefficients can also become prohibitive when a large number of uncertain parameters is involved.

## References

- [1] R.R. Craig and M.C.C. Bampton. Coupling of Substructures for Dynamic Analyses. *AIAA Journal*, 6(7):1313–1319, 1968.
- [2] *Dynamic Model Reduction Methods*, pages 265–280. Springer Berlin Heidelberg, Berlin, Heidelberg, 2008.
- [3] B.R. Mace, K. Worden, and G. Manson. Uncertainty in structural dynamics. *Journal of Sound and Vibration*, 288(3):423 – 429, 2005. Uncertainty in structural dynamics.
- [4] G.I. Schuëller. On the treatment of uncertainties in structural mechanics and analysis. *Computers & Structures*, 85(5):235 – 243, 2007. Computational Stochastic Mechanics.
- [5] Kieu, D.T., Bergeot, B., Gobert, M.-L., and Berger, S. Stability analysis of a clutch system with uncertain parameters using sparse polynomial chaos expansions. *Mechanics & Industry*, 20(1):104, 2019.
- [6] G. Blatman and B. Sudret. Anisotropic parcimonious polynomial chaos expansions based on the sparsity-of-effects principle. In *Proc ICOSSAR’09, International Conference in Structural Safety and Reliability*, 2009.
- [7] G. Blatman and B. Sudret. An adaptive algorithm to build up sparse polynomial chaos expansions for stochastic finite element analysis. *Probabilistic Engineering Mechanics*, 25(2):183–197, 2010.
- [8] G. Blatman and B. Sudret. Sparse polynomial chaos expansions and adaptive stochastic finite elements using a regression approach. *Comptes Rendus Mécanique*, 336(6):518 – 523, 2008.
- [9] M.H. Trinh, S. Berger, and E. Aubry. Stability analysis of a clutch system with multi-element generalized polynomial chaos. *Mechanics & Industry*, 17(2):205, 2016.
- [10] D. Xiu and G.E. Karniadakis. The wiener–askey polynomial chaos for stochastic differential equations. *SIAM Journal on Scientific Computing*, 24(2):619–644, 2002.
- [11] R.H. Cameron and W.T. Martin. The orthogonal development of non-linear functionals in series of fourier-hermite functionals. *Annals of Mathematics*, 48(2):385–392, 1947.
- [12] R. Askey and J.A. Wilson. *Some basic hypergeometric orthogonal polynomials that generalize Jacobi polynomials*, volume 319. American Mathematical Soc., 1985.
- [13] D. Xiu and G.E. Karniadakis. Modeling uncertainty in steady state diffusion problems via generalized polynomial chaos. *Computer Methods in Applied Mechanics and Engineering*, 191(43):4927–4948, 2002.
- [14] M.D. McKay, R.J. Beckman, and W.J. Conover. A comparison of three methods for selecting values of input variables in the analysis of output from a computer code. *Technometrics*, 21(2):239–245, 1979.
- [15] M. Berveiller, B. Sudret, and M. Lemaire. Stochastic finite element: a non intrusive approach by regression. *European Journal of Computational Mechanics/Revue Européenne de Mécanique Numérique*, 15(1-3):81–92, 2006.
- [16] B. Sudret. Global sensitivity analysis using polynomial chaos expansions. *Reliability Engineering & System Safety*, 93(7):964 – 979, 2008. Bayesian Networks in Dependability.
- [17] G. Blatman. *Adaptive sparse polynomial chaos expansions for uncertainty propagation and sensitivity analysis*. PhD thesis, Université BLAISE PASCAL - Clermont II, 2009.
- [18] G.G. Wang. Adaptive response surface method using inherited Latin Hypercube design points. *Journal of Mechanical Design*, 125(2):210–220, 2003.